doi: 10.1016/S0022-2836(02)00023-2 available online at http://www.idealibrary.com on IDEAL® J. Mol. Biol. (2002) 318, 429–442

JMB

Knowledge-based Design of Reagentless Fluorescent Biosensors from Recombinant Antibodies

Martial Renard[1], Laurent Belkadi[1], Nicolas Hugo[2], Patrick England[1] Danièle Altschuh[2] and Hugues Bedouelle[1]*

[1]*Département de Biologie Structurale et Chimie CNRS URA 2185, Institut Pasteur, 28 rue Docteur Roux 75724 Paris Cedex 15, France*

[2]*CNRS UMR 7100, Ecole Supérieure de Biotechnologie de Strasbourg, Pôle API Bld Sébastien Brant 67400 Illkirch, France*

**Corresponding author*

The possibility of obtaining from any antibody a fluorescent conjugate which responds to the binding of the antigen by a variation of its fluorescence, would be of great interest in the analytical sciences and for the construction of protein chips. This possibility was explored with antibody mAbD1.3 directed against hen egg white lysozyme. Rules of design were developed to identify the residues of the antibody to which a fluorophore could be chemically coupled, after changing them to cysteine by mutagenesis. These rules were based on: the target residue belonging to a topological neighbourhood of the antigen in the structure of the complex between antibody and antigen; its absence of functional importance for the interaction with the antigen; and its solvent accessibility in the structure of the free antibody. Seventeen conjugates between the single-chain variable fragment scFv of mAbD1.3 and an environment-sensitive fluorophore were constructed. For six of the ten residues which fully satisfied the design rules, the relative variation of the fluorescence intensity between the free and bound states of the conjugate was comprised between 12 and 75% (in non-optimal buffer), and the affinity of the conjugate for lysozyme remained unchanged relative to the parental scFv. In contrast, such results were true for only one of the seven residues which failed to satisfy one of the rules and were used as controls. One of the conjugates was studied in more detail. Its fluorescence increased proportionally to the concentration of lysozyme in a nanomolar range, up to 90% in a defined buffer, and 40% in serum. This increase was specific for hen egg lysozyme and it was not observed with a closely related protein, turkey egg lysozyme. The residues which gave operational conjugates (six in V_L and one in V_H), were located in the immediate vicinity of residues which are functionally important, along the sequence of FvD1.3. The results suggest rules of design for constructing antigen-sensitive fluorescent conjugates from any antibody, in the absence of structural data.

Keywords: antigen; biosensor; fluorophore; immunosensor; protein design

Introduction

A biosensor comprises two major components: a biological receptor, which specifically recognizes a ligand; and a transducer, which detects the recognition event and transforms it into a measurable signal. Four main types of tranducers, which exploit changes in the optical, electrochemical, mass or heat properties, are used in the technologies of biosensors.[1,2] A biosensor functions reagentless if the different steps going from the ligand recognition to the signal measurement do not imply any change in its composition. This characteristic is necessary for a continuous measurement.

The monoclonal antibodies seem ideally suited to provide the biological receptor of biosensors, since they can be directed against most haptens or

Abbreviations used: Fv, variable fragment; scFv, single chain Fv; mAbD1.3, monoclonal antibody D1.3; FvD1.3 and scFvD1.3, Fv and scFv derived from mAbD1.3; HEL, hen egg white lysozyme; TEL, turkey lysozyme; IANBD ester, (*N*-((2-(iodoacetoxy)ethyl)-*N*-methyl)amino-7-nitrobenz-2-oxa-1,3-diazole; ASA, solvent accessible surface area; CSA, solvent contact surface area; SE, standard error.

E-mail address of the corresponding author: hbedouel@pasteur.fr

0022-2836/02/$ - see front matter

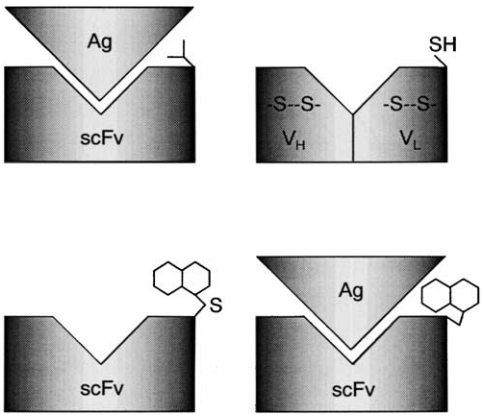

Figure 1. Construction of a reagentless fluorescent biosensor from an antibody fragment. Top left. A residue, close to the paratope but non-essential for the interaction with the antigen, is identified. Top right. This residue is mutated into a cysteine. Bottom left. A fluorophore, sensitive to its micro-environment, is coupled to the reduced thiol group without altering the disulphide bonds of the antibody fragment. Bottom right. The binding of the antigen modifies the environment of the fluorophore and leads to a change in its fluorescence.

macromolecules. However, they are not well adapted to the simple mechanisms of signal transduction. Several proposals have been made to solve this problem. North[3] has proposed the insertion of a reporter group close to the paratope (binding-site) of the antibody, for example fluorophores or luminophores which are particularly sensitive to subtle changes in their electronic environment. Schultz and co-workers[4] proposed oligonucleotide-directed mutagenesis to introduce a nucleophilic cysteine residue in a specific site of the antibody paratope, chosen on the basis of the crystal structure, then to couple chemically a reactive fluorophore to this mutant Cys residue (Figure 1). This approach was used to transform other types of proteins into biosensors, e.g. the *Escherichia coli* binding proteins for phosphate,[5] maltose,[6] and glucose,[7] or the B1 domain of the streptococcal protein G.[8]

This approach has never been used to transform antibodies into biosensors, we suspect for the following reason. The receptors studied so far did not contain any Cys residue. In contrast, the recombinant antibodies and in particular their variable fragments, which can be easily produced and engineered, contain disulphide bridges which are essential for their thermodynamic stability,[9] and could be attacked and reduced during the coupling of the fluorophore. Except for the Cys residues which are engaged in the two disulphide bonds, antibody-variable fragments rarely contain Cys residues, in particular within or in the neighbourhood of the hypervariable loops.[10] Their rarity suggests that such residues could be incompatible with the folding or function of antibodies. The antibodies and their fragments must be produced in an oxidizing cellular compartment so that their disulphide bridges can form, for example in the periplasm of *E. coli* cells.[11] Under these conditions, it is unlikely that an unpaired Cys residue will be in the reduced state which is necessary for its chemical coupling with a fluorophore. Finally, the site of coupling must be chosen in such a way that the binding of the antigen modifies the environment and the fluorescence of the fluorophore but does not compromise the interaction between antibody and antigen. To our knowledge, no one has solved this set of problems.

Here, we show that these difficulties can be overcome. We formalized rules of design to choose the sites of fluorophore coupling on an antibody, from the structure of the complex with its antigen and functional data on their interaction. We applied these rules to the single-chain variable-fragment (scFv) of antibody mAbD1.3, which is directed against hen egg white lysozyme (HEL) and for which numerous structural and mutagenesis data are available.[12–19] We constructed ten fluorescent conjugates from residues of scFvD1.3 which satisfied the design criteria fully, and seven conjugates from residues which failed to satisfy one of them and were used as controls. The chosen residues were changed into Cys by mutagenesis and the mutant scFvD1.3 fragments were produced in the periplasm of *E. coli* cells. A mild reduction was sufficient to reactivate the mutant Cys residue and then to couple it with IANBD, an environment-sensitive fluorophore, without disrupting the essential disulphide bonds of the scFv. We measured and compared the variations of fluorescence for the conjugates upon HEL binding, and the kinetic parameters of interaction with HEL for the mutant scFvD1.3 fragments and their conjugates. We found seven operational conjugates. The fluorescence intensity of one of them, studied in more detail, increased strongly upon binding of HEL and this increase enabled its titration. The construction of these immuno-sensors did not exploit any specific property of the chosen scFv and its principle could therefore be generalized to other antibodies. The location of the sites which gave operational conjugates suggested more general rules of design, valid even in the absence of the structure of the complex between antibody and antigen.

Results

Search for coupling sites

To identify sites of coupling for a fluorophore within the FvD1.3 fragment, we used the available crystallographic and mutational data on its interaction with HEL. The crystal structures of the free FvD1.3 and of the FvD1.3:HEL complex have been solved.[12] However, to simplify the procedure of identification and generalize it more easily to molecules for which only the structure of the complex is available, we did not use the crystal

Table 1. Identification of peripheral sites for the coupling of fluorophores

Residue	Radius (Å)	Mutations	$\Delta\Delta G$ (kcal mol^{-1})	CSA (%)	Choice	Comment
L-Asn28	2.0	na	na	nc	−	Distance
L-His30	d	A	0.8	17.5	+	
L-Asn31	2.0	na	na	40.4	−, *	Distance
L-Tyr32	d	A, F	1.7, 2.2	nc	−	Affinity
L-Tyr49	d	A	0.8	10.9	+	
L-Tyr50	d	A, F, N	0.5, 0.5, 2.3	17.6	−, *	Affinity
L-Thr52	1.4	K	0.0	64.1	+	
L-Thr53	d	A	−0.2	27.0	+	
L-Asp56	2.6	na	na	100.0	−, *	Distance
L-Gly68	2.9	na	na	nc	−	Distance
L-Phe91	b	na	na	nc	−	Backbone
L-Trp92	d	A, D	3.7, 4.1	23.6	−, *	Affinity
L-Ser93	d	A	0.3	57.1	+	
L-Thr94	i, 1.7	na	na	47.3	+	
H-Phe27	2.9	N(+E46Q)	1.1	nc	−	Distance
H-Ser28	2.0	na	na	52.3	−, *	Distance
H-Thr30	i, 1.4	A	0.1	70.2	+	
H-Gly31	d	na	na	24.1 (C^{α})	+	
H-Tyr32	d	A, F	(0.5, 1.1), 0.4	12.9	+	
H-Gly33	1.4	na	na	nc	−	
H-Trp52	d	A	0.4, 0.9	nc	−	Affinity
H-Gly53	d	na	na	0.0 (C^{α})	−, *	Accessibility
H-Asp54	d	A	1.7	nc	−	Affinity
H-Asn56	2.3	A, S	0.2, 0.2	80.2	−, *	Distance
H-Asp58	1.7	A	−0.2	nc	−	Distance
H-Arg97	2.3	na	na	nc	−	Distance
H-Arg99	d	A	0.1	38.2	+	
H-Asp100	d	A, N	3.1, 3.7	nc	−	Affinity
H-Tyr101	d	A, F	>4, 2.5	nc	−	Affinity
H-Arg102	d	K, M	1.6, 3.2	nc	−	Affinity

Column 1, residues located in the neighbourhood of HEL in the structure of the FvD1.3:HEL complex. H, heavy chain; L, light (κ) chain. Column 2, radius of the sphere of solvent for which the ASA of the residue in column 1 is modified by the binding of HEL. The following values were used: 1.4, 1.7, 2.0, 2.3, 2.6 and 2.9 Å. d, residue in direct contact with HEL through side-chain atoms; b, direct contact through a backbone atom (the side-chain of L-Phe91 is fully buried in the structure of FvD1.3); i, indirect contact through a water molecule. Columns 3 and 4, known mutations of the residue in column 1 and the associated variations of the free energy of interaction with HEL.[12–19] Column 5, CSA of either the S^{γ} atom of the mutant Cys or the C^{α} atom of the wild-type Gly in the free state of FvD1.3. In the former case, the CSA was calculated from a model of the mutant FvD1.3 fragment and in the latter case, from the crystal structure of the wild-type FvD1.3. Column 6, decision about the use of the residue as a coupling site. (−) Rejection; (+), selection; (*), use as a control. Column 7, reason for the decision. na, not available; nc, not calculated.

structure of free FvD1.3. Instead, we obtained a structural model of free FvD1.3 by deleting the crystallographic coordinates of HEL in the structure of the complex. We used three criteria.

(1) The target site on the antibody must be close to the antigen in their complex. We searched for the residues of FvD1.3, which are in direct contact with HEL, those which are in contact by the intermediate of a water molecule, and those whose solvent accessible surface area (ASA) is modified by the binding of HEL when one uses a sphere of radius (r) between 1.4 Å and 2.9 Å as a solvent molecule. The use of radii larger than that of a water molecule, 1.4 Å, enables one to define an enlarged neighbourhood of the antigen at the surface of the antibody and to take into account the larger volume of a fluorophore, compared to a water molecule (Table 1, columns 1 and 2). (2) The change of the target residue into a cysteine and the coupling of a fluorophore must not be deleterious for the interaction between the antibody and the antigen. We used the available mutagenesis data to exclude the residues of FvD1.3 where one of the mutations results in a variation of the free energy of interaction with HEL greater than 0.8 kcal mol^{-1} (Table 1, columns 3 and 4). This criterion should ensure that the target residue is peripheral rather than central relative to the interface between antibody and antigen, and that the fluorescent conjugate will keep a good affinity for the antigen. (3) The mutant Cys residue must be readily coupled to the fluorophore. *A priori*, this condition implies that its S^{γ} atom must be accessible to the solvent in the structure of the mutant antibody fragment, taken in its free state. For each site which satisfied conditions (1) and (2) above and whose wild-type residue was neither Ala nor Gly, we constructed a structural model of the mutant FvD1.3 fragment and calculated the solvent contact surface area (CSA) of the mutant S^{γ} atom in the model. When the wild-type residue was Gly, we calculated the CSA of its C^{α} atom in the structure of the free FvD1.3 (Table 1, column 5).

Note that our three criteria of design were quantitative and thus amenable to validation or falsification. In that respect, they clearly differed from those used by others to construct a fluorescent conjugate from the B1 domain of the streptococcal

Table 2. Effect of the concentration of 2-mercaptoethanol on the efficiency of coupling between thiol-reactive fluorophores and the L-S93C mutant

2-Mercaptoethanol (mM)	Fluorophore	Coupling yield (%)	Protein yield (%)
50	IANBD	>168	4
10	IANBD	83	9
10	CNBD	95	16
10	Acrylodan	79	12
10	5-IAF	nd	11
1.0	IANBD	34	12
0.1	IANBD	26	15
0	IANBD	8	85

The scFvD1.3(L-S93C) preparation (100 μg, 1 ml) was treated with the indicated concentration of 2-mercaptoethanol, dessalted and mixed immediately with the fluorophore. The coupling yield (% of fluorophore molecule/scFv molecule) and the protein yield (% of protein remaining soluble after the entire coupling procedure) were determined as described in Materials and Methods. nd, not determined. Acrylodan, 6-acryloyl-2-dimethylaminonaphtalene; CNBD, 4-chloro-7-nitrobenz-2-oxa-1,3-diazole; 5-IAF, 5-iodoacetamidofluorescein; IANBD ester, (*N*-((2-(iodoacetoxy)ethyl)-*N*-methyl)amino-7-nitrobenz-2-oxa-1,3-diazole.

protein G. In this case, residues of the B1 domain were considered as peripheral relative to its interface with the Fc fragment of the human IgG on the sole basis of a visual inspection of the complex structure.[8] Among the sites which satisfied our three criteria of design, we privileged those in direct contact with the antigen through their side-chains (L-His30, L-Tyr49, L-Thr53, L-Ser93, H-Gly31, H-Tyr32, H-Arg99), those in indirect contact through a water molecule (L-Thr94, H-Thr30), and those in the immediate neighbourhood of the antigen (L-Thr52). As controls, we studied a few sites located in an enlarged neighbourhood of the antigen (L-Asn31, L-Asp56, H-Ser28, H-Asn56), a Gly residue (H-Gly53) whose C^{α} atom is totally buried, and two aromatic residues which are important for the interaction with the antigen (L-Tyr50 and L-Trp92). We wanted to test if the aromatic ring of the fluorophore could restore some of the interactions between HEL and the aromatic side-chains of the wild-type FvD1.3.

Coupling necessitates reactivation by a mild reduction

We chose residue L-Ser93 to establish the conditions for the construction of the fluorescent conjugates. Residue L-Ser93 of the wild-type scFvD1.3(wt) was mutated to Cys. The mutant scFvD1.3(L-S93C) fragment was produced in the periplasm of *E. coli* cells and purified through its hexahistidine affinity tag. The reactions between various fluorescent compounds, including IANBD ester, and fresh preparations of scFvD1.3(L-S93C) gave low yields of coupling. Two hypotheses could explain this result. The mutant Cys residues of two scFv molecules could associate to form an intermolecular disulphide bridge and thus loose

Table 3. Production yield and fluorescence of the conjugates

Residue	Radius (Å)	*f*(Cys) (10^{-4})	Production (μg l^{-1})	Reaction yield (%)	Coupling yield (%)	*E* (%)
wt	na	na	637 ± 88	41	<8	0
L-His30	d	6.5	83 ± 49	11	116	+7
L-Asn31*	2.0	2.2	232 ± 124	7	103	+16
L-Tyr49	d	15.5	202	20	78	+75
L-Tyr50*	d	4.4	221	33	88	+1
L-Thr52	1.4	4.4	427 ± 204	24	83	+12
L-Thr53	d	2.2	325 ± 72	43	104	+13
L-Asp56*	2.6	6.7	350	35	116	−1
L-Trp92*	d	19.0	430 ± 47	43	107	+53
L-Ser93	d	6.3	513 ± 73	9	83	+26
L-Thr94	i, 1.7	25.4	272 ± 45	24	94	+55
H-Ser28*	2.0	2.4	166	15	111	−2
H-Thr30	i, 1.4	7.1	420	19	72	−6
H-Gly31	d	14.1	208	16	130	−2
H-Tyr32	d	48.1	60 ± 5	12	85	+26
H-Gly53*	d	10.5	658	46	42	+1
H-Asn56*	2.3	11.5	409	23	92	+5
H-Arg99	d	115.1	128	14	101	−6

Column 1, site of coupling. (*), sites used as controls. Column 2, identical to column 2 of Table 1. Column 3, frequency of a Cys residue at the same position in all the V_{κ} or V_H sequences of the Kabat database.[10] Column 4, purification yield of the scFvD1.3 mutant, carrying a change of the residue of column 1 to Cys, under standardized conditions and per litre of culture. Column 5, protein yield of the reaction steps going from the purified mutant to the conjugate. Column 6, number of molecules of IANBD/molecule of scFv after coupling. Column 7, relative variation of the conjugate fluorescence at 535 nm between its free and HEL bound states in 100 mM imidazole and buffer A at 25 °C. na, not applicable.

Table 4. Parameters of interaction between the scFvD1.3 mutants and HEL

Mutation	k_{on} (10^5 M^{-1} s^{-1})	k_{off} (10^{-3} s^{-1})	K'_D (nM)	$\Delta\Delta G$ (kcal mol^{-1})
wt	3.1 ± 0.5	4.5 ± 0.1	16 ± 3	0.0 ± 0.1
L-Y49C	5 ± 4	2.6 ± 0.5	12 ± 9	−0.3 ± 0.6
L-T52C	5.7 ± 0.5	2.2 ± 0.4	3.9 ± 0.3	−0.8 ± 0.1
L-T53C	5 ± 3	6.3 ± 0.9	18 ± 9	0.0 ± 0.4
L-W92C	nm	nm	nm	>3
L-S93C	6 ± 1	5.6 ± 0.8	9.4 ± 0.5	−0.3 ± 0.1
L-T94C	5.0 ± 0.2	2.4 ± 0.3	4.9 ± 0.4	−0.7 ± 0.1

The association and dissociation rate constants, k_{on} and k_{off}, for immobilized HEL and their ratio $K'_D = k_{off}/k_{on}$ were measured with the Biacore apparatus in buffer D at 25 °C, as described in Materials and Methods. The interaction energy between each scFv derivative and HEL was calculated by the relation $\Delta G = RT \ln(K'_D)$, and the variation of interaction energy resulting from a mutation by $\Delta\Delta G = \Delta G(\text{mut}) - \Delta G(\text{wt})$. The standard error (SE) on $\Delta\Delta G$ was calculated from the standard errors on ΔG(wt) and ΔG(mut) through the formula $[SE(\Delta\Delta G)]^2 = [SE(\Delta G(\text{mut}))]^2 + [SE(\Delta G(\text{wt}))]^2$. mut, mutant; wt, wild-type; nm, the dissociation rate was too fast to be measured. Each entry gives the average value and the associated SE of at least two independent experiments.

their reactivity. Alternatively, the mutant Cys residue could be oxidized, either by molecular oxygen or by conjugation with a thiol-containing compound of the periplasm. The behaviour of the wild-type and mutant scFv fragments (1.5 μM) were analysed in experiments of size exclusion chromatography to distinguish between these two hypotheses. scFvD1.3(L-S93C) ran as a pure monomer in these experiments whereas scFvD1.3(wt) ran mainly as a monomer but with a small proportion (18%) of dimeric molecules, most likely in the form of diabodies (results not shown).[20] Thus, scFvD1.3(L-S93C) did not form dimers through intermolecular disulphide bridges.

We treated scFvD1.3(L-S93C) with various reducing agents to restore the reactivity of the mutant Cys residue towards the IANBD ester. We found that 2-mercaptoethanol denatured and precipitated part of the scFvD1.3(L-S93C) molecules in a concentration-dependent manner, probably by disrupting their essential disulphide bridges. However, the molecules that remained soluble, could react with the IANBD ester (Table 2). The coupling between scFvD1.3(L-S93C) and IANBD, to give the conjugate scFvD1.3 (L-S93ANBD), was 83% efficient and thus nearly stoichiometric after treatment with 10 mM 2-mercaptoethanol during one hour at room temperature. We could obtain conjugates between scFvD1.3 (L-S93C) and other fluorophores (CNBD, acrylodan and 5-IAF) under the same conditions, which were therefore used in the remainder of the work (Table 2). In contrast, we found that phosphines totally denatured scFvD1.3(L-S93C).

Construction of the scFv–ANBD conjugates

For each of the 17 selected positions, the wild-type residue was mutated to Cys. Most of the mutant derivatives of scFvD1.3 were produced in good yields (Table 3, column 4). The mild reduction by 2-mercaptoethanol and the coupling with IANBD denatured part of the molecules, so that <46% of the starting materials remained soluble (Table 3, column 5). A yield >40% was obtained for the wild-type scFvD1.3 and for a few mutants (L-T53C, L-W92C, H-G53C). All the other mutants were more affected by 2-mercaptoethanol than the wild-type, but less than the L-S93C mutant, which was used for establishing the coupling conditions. We observed a weak but significant correlation between the yield of production and the resistance to the reducing and coupling treatments (Table 3, columns 4 and 5; $R = 0.6$).

To verify the specificity of the coupling, we separated scFvD1.3 and its derivatives from the unreacted IANBD ester by chromatography on a Ni^{2+} column, then recorded the absorbance spectra of the purified materials. The spectra of the materials derived from the scFvD1.3 mutants showed a peak of absorbance, located around 500 nm and corresponding to the fluorophore, which was absent from the spectrum of the

Table 5. Parameters of interaction between the fluorescent conjugates and HEL

Position	k_{on} (10^5 M^{-1} s^{-1})	k_{off} (10^{-3} s^{-1})	K'_D (nM)	$\Delta\Delta G$ (kcal mol^{-1})
L-His30	5.6	6.9	12	−0.1
L-Tyr49	1.1	1.7	16	0.0
L-Thr52	4.5 ± 0.5	3.4 ± 0.2	7.7 ± 0.4	−0.4 ± 0.1
L-Thr53	6 ± 2	5.7 ± 0.4	10 ± 3	−0.3 ± 0.2
L-Trp92	nm	nm	nm	>3
L-Ser93	3.8 ± 0.6	5.6 ± 0.2	15 ± 2	0.0 ± 0.1
L-Thr94	2.5 ± 0.2	3.4 ± 0.3	13.7 ± 0.1	−0.1 ± 0.1
H-Tyr32	2.8	5.9	21	+0.2

See the legend to Table 4.

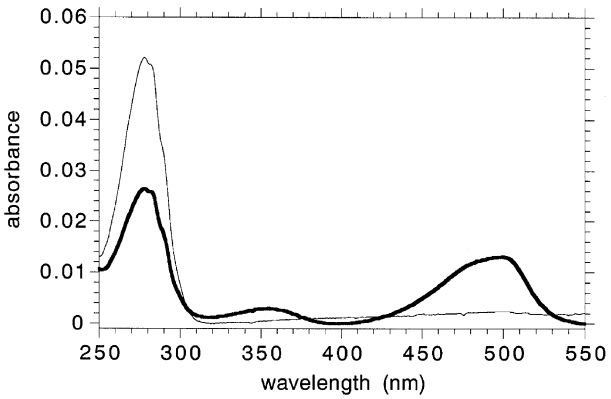

Figure 2. Absorbance spectra of scFvD1.3 derivatives after reaction with IANBD. scFvD1.3(wt) and scFvD1.3 (L-S93C) were reduced under mild conditions, reacted with IANBD, then separated from unreacted IANBD. The protein absorbed around 280 nm and the fluorophore around 500 nm in buffer A with 100 mM imidazole. Thin line, scFvD1.3(wt); thick line, scFvD1.3 (L-S93ANBD).

materials derived from scFvD1.3(wt) (Figure 2). From these spectra, we could calculate that the yield of IANBD coupling (number of coupled IANBD molecules per scFv molecule) was close to 1:1, except for the H-G53C mutant (Table 3, column 6). The characterization of the scFv–ANBD conjugates was therefore performed on molecular species that were fully coupled, except in one case.

The mass of scFvD1.3(wt), measured by spectrometry (Materials and Methods), was in conformity with its sequence (calculated, 26,795.62; measured, 26,796(±2)). The mass of scFvD1.3 (L-S93C) showed an excess of 80 units relative to the theoretical mass (calculated, 26,811.67, measured, 26,892(±2)). This excess suggested that the mutant Cys residue reacted with a periplasmic component during the production of scFvD1.3 (L-S93C), and thus provided an explanation for the lack of coupling between the IANBD ester and a non-reduced scFvD1.3(L-S93C). This component could be cysteamine (decarboxycysteine, 77.12 mass units), given the observed mass excess. The mass of the scFvD1.3(L-S93ANBD) conjugate confirmed the covalency of its coupling with the IANBD ester and the presence of only one molecule of fluorophore per molecule of scFv (calculated, 27,089.90; measured, 27,090(±1)). This mass analysis also showed that the molecules of scFvD1.3(L-S93C) did not form mixed disulphides with 2-mercaptoethanol.

Variation of fluorescence on antigen binding

The fluorescence intensity (I) of the scFvD1.3–ANBD conjugates, excited at 480 nm, was measured in the presence of a saturating concentration of HEL or in its absence. The maximal value of I was attained for an emission wavelength, which depended slightly on the particular conjugate and was between 536.0 and 538.0 nm. The wavelength of this maximum shifted by <3 nm between the free and bound states of the conjugate in all cases. The relative variation of I at 535 nm, given by $E = (I_b - I_f)/I_f$ where I_f and I_b are the values for the free and bound conjugates, was between a decrease of -6% and an increase of $+75\%$ for the different conjugates (Table 3, column 7). The highest values of E were obtained for coupling residues which were in contact with HEL, either directly or through a water molecule, in the structure of the FvD1.3:HEL complex. Lower values of E were obtained for coupling residues which were not in contact with HEL but were located in a narrow neighbourhood, defined by a sphere of solvent with $1.4\ \text{Å} \le r \le 2.0\ \text{Å}$. Finally, the values of E became negligible for neighbourhoods defined by $r > 2.0$ Å. Residues L-Tyr50 and L-Trp92 of FvD1.3 are strongly and directly involved in the interaction with HEL (Table 1). In particular, L-Tyr50 results from the hypersomatic maturation of antibody mAbD1.3.[19] The results were very different for these two residues, used as controls. L-Tyr50 gave a conjugate with a negligible E value (1%) whereas L-Trp92 gave a conjugate with a high E value (53%).

We observed that the relative variations of fluorescence intensity, E, for the scFvD1.3–ANBD conjugates depended on the buffer used, but not their classification according to the E values. For example, we found $E = 90\%$ for scFvD1.3(L-S93ANBD) in buffer B and $E = 26\%$ in buffer A containing 100 mM imidazole. The conjugates of scFvD1.3(L-S93C) with fluorophores other than IANBD, did not show significant variations of fluorescence on the binding of HEL (Table 2). We used only IANBD in our study for this reason.

Parameters of interaction between the scFv1.3 derivatives and HEL

We determined the effects of the mutation to Cys and of the coupling with IANBD on the parameters of interaction between scFvD1.3 and HEL, for the sites which led to a value $E > 10\%$. The rate constants of association k_{on} and of dissociation k_{off} between the derivatives of scFvD1.3 and immobilized HEL were measured by Biacore. The effects of the mutations to Cys on the affinity were weak, except for the control mutation L-W92C (Table 4). The analysis of the Biacore sensorgrams showed a very rapid dissociation between the scFvD1.3 (L-W92C) mutant and HEL, consistent with the important contribution of residue L-Trp92 to the interaction energy between FvD1.3 and HEL. Mutations L-T52C and L-T94C had weak but significant effects: k_{on} was increased and k_{off} was decreased, which resulted in a three- to fourfold lower constant of dissociation K'_d between the mutant scFvD1.3 and immobilized HEL.

A comparison of the kinetic parameters for the mutant scFvD1.3 fragments and for their fluorescent derivatives showed that the presence of the fluorophore had very little effect on the interaction

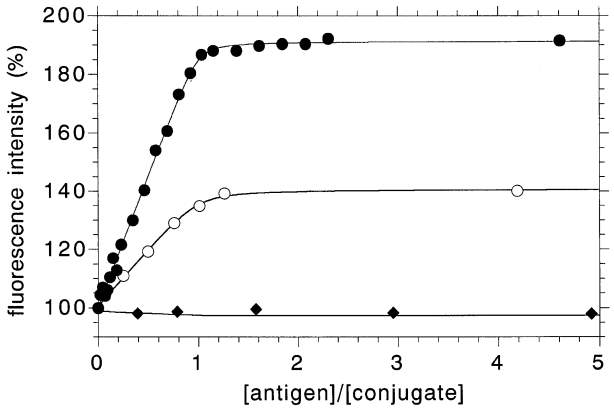

Figure 3. Titration of HEL and TEL by the scFvD1.3 (L-S93ANBD) conjugate, in buffer B or serum at 25 °C, as monitored by fluorescence. The fluorescence intensity of the reaction mixture (1 ml) was measured at 535 nm then normalized to the intensity of the free scFv conjugate. It is given as a function of the ratio [antigen]/[conjugate] for simplicity. The continuous curves were obtained by fitting equations similar to that given in Materials and Methods, to the experimental data. (●) HEL in buffer B; (◆) TEL in buffer B; (○) HEL in serum.

with HEL (Table 5). For positions L-52 and L-94, the coupling of the fluorophore shifted the values of the kinetic parameters back to those of the wild-type scFvD1.3. Therefore, the mutation to Cys perturbed more the affinity than the mutation and the coupling of IANBD together. The coupling of IANBD to the scFv(L-W92C) mutant did not restore its affinity for HEL, even though the NBD and indol rings are structurally close.

Properties of scFvD1.3(L-S93ANBD) as a biosensor

We characterized the properties of the scFvD1.3(L-S93ANBD) conjugate as a biosensor in more detail. For this, we recorded its spectra of fluorescence emission in the presence of increasing concentrations of HEL, either in a defined buffer (buffer B) or in a complex mixture of molecules (calf serum). We observed an increase in the intensity of the conjugate fluorescence in both cases, and a slight but significant shift of the wavelength of maximal emission in buffer B, from 535.5(±0.1) to 538.4(±0.1) nm. The titration curve of the conjugate (500 nM total concentration), monitored by the intensity of fluorescence at 535 nm in buffer B, was linear between 0 and 400 nM HEL, with a detection threshold of 10 nM (0.12 ppm; Figure 3). The theoretical equation which links the fluorescence intensity and the concentration of HEL was fitted to the experimental data, with K_D, the concentration of functional scFv conjugate, the molar fluorescence of the free conjugate, and the molar fluorescence of its complex with HEL as fitting parameters. In buffer B, the complex had a higher fluorescence intensity than the free conjugate, by 91(±2)%. The value of K_D obtained by this method, 2 nM, with high concentrations of total conjugate (500 nM) and HEL (10–5000 nM), was consistent with the value 6.5(±0.2) nM, determined by competition Biacore under more satisfying experimental conditions (Table 6). The proportion of functional molecules of conjugate, obtained by the titration method, was equal to 82(±2)% and therefore also consistent with the value obtained by Biacore, 86(±10)% (Table 6).

The titration curves of the scFvD1.3(L-S93ANBD) conjugate were similar in calf serum and in buffer B (Figure 3). Thus, this type of biosensor could be used in a complex mixture such as a body fluid. The relative increase in fluorescence on HEL binding was lower in serum than in buffer B (40% *versus* 91%). To explain this difference, we compared the molar fluorescences of the free scFvD1.3(L-S93ANBD) conjugate and of its complex with HEL, in serum and in buffer B. We observed that the fluorescence was quenched in serum relative to buffer B, and that the quenching was greater for the bound than for the free scFv conjugate (2.0 *versus* 1.5-fold). Therefore, the lower variation of fluorescence in serum was due to differential quenching. We found that the dissociation constants K_D between the scFvD1.3 (L-S93ANBD) conjugate and HEL, measured by competition Biacore, were very close in serum (4.2(±0.1) nM) and in buffer E (6.5(±0.2) nM). Thus, the components of serum did not affect the interaction between the scFv conjugate and HEL, and the mechanism of the fluorescence quenching remains unknown.

Table 6. Dissociation constants in solution

scFv	Activity (%)	K_D(HEL) (nM)	K_D(TEL) (μM)
wt	44 ± 7	5.9 ± 0.2	5.5 ± 0.2
L-S93C native	18 ± 5	12.3 ± 0.5	3.9 ± 0.1
L-S93C reduced	52 ± 9	14.4 ± 0.3	nd
L-S93ANBD	86 ± 10	6.5 ± 0.2	3.6 ± 0.2

K_D, between scFvD1.3 derivatives and either HEL or TEL, as measured by competition Biacore at 25 °C in buffer E. Column 1, native, before reduction with 2-mercaptoethanol; reduced, after this reduction. Column 2, ratio between the concentrations of active sites and protein, as measured by the flow method and $A_{280\ nm}$, respectively; mean ± standard error (SE) for experiments performed at seven different concentrations of HEL. Columns 3 and 4, value of K_D and associated SE in the fitting of the equilibrium equation to the raw experimental data. See Materials and Methods for details.

Specificity of the scFvD1.3(L-S93ANBD) biosensor

The experiments of HEL titration by the scFvD1.3(L-S93ANBD) conjugate in serum, a complex mixture, showed that their recognition was specific. To further establish this specificity, we titrated the turkey egg white lysozyme (TEL) with the scFvD1.3(L-S93ANBD) conjugate in buffer B

(Figure 3). TEL and HEL are homologous proteins whose sequences differ in only seven positions. The affinities of TEL for the molecules of scFvD1.3(wt), scFvD1.3(L-S93C) and scFvD1.3 (L-S93ANBD) varied between 3.5 and 5.5 μM (Table 6), consistent with those published for the FvD1.3 fragment (1.4 μM).[21] The fluorescence of the scFvD1.3(L-S93ANBD) conjugate did not show any variation on the binding of TEL, even at saturating concentrations (>50 μM). Thus, the scFv conjugate appeared infinitely more specific for HEL than for TEL when the formation of the complex was monitored by fluorescence, and only 550-fold more specific when the K_D values were determined by competition Biacore. The lack of fluorescence signal upon interaction between the scFv conjugate and TEL was not due to a trivial cause like the inactivity of either the conjugate or TEL molecules, because the fluorescence and Biacore experiments were done with the same preparations. Rather, this lack could be due to a conformational change of the scFv conjugate. Residue 121 of lysozyme is indeed Gln in HEL and His in TEL. The structure of the FvD1.3:HEL complex shows that Gln121 makes a pair of hydrogen bonds with the L-Ser93-N and L-Phe91-O atoms of the V_L main-chain. The structure of the Fv-D1.3:TEL complex shows that His121 makes only one hydrogen bond with the L-Trp92-O atom and that there is an important conformational change of the peptide torsion angles for residues L-Trp92 and L-Ser93. This change makes the side-chain of L-Ser93, which is the site of fluorophore coupling, rotate from a position which is close to HEL, to a position which is far from TEL.[21] This conformational change could explain the total lack of response of the scFv conjugate to the binding of TEL.

Discussion

Production yield and stability of the mutant scFv fragments

We changed 17 residues of the scFvD1.3 fragment to Cys and expressed the mutant fragments in the periplasm of *E. coli* cells. The production yields of the mutants varied up to tenfold. These variations could be due to a defective folding or stability of some mutants, which would lead to their aggregation. The mutations changed residues which are both in the hypervariable regions (CDR) as defined by Kabat & Wu,[10] and in the hypervariable structural loops (L and H) as defined by Chothia and co-workers,[22] except L-Asp56 which is within CDR2 but outside of L2, and L-Tyr49 which is outside of both CDR2 and L2. None of the mutated residues was determining for the canonical conformation of the loops.[22–25] Therefore, the mutations to Cys ought not to change strongly the conformational stability of the hypervariable loops or polypeptide scaffold on structural grounds, except maybe for L-Y49C, since residue L-49 is preferentially Tyr in the κ-chains.[10] Cys residues are naturally found in V_κ and V_H sequences at the positions which were mutated in this study. However, their very low frequencies (Table 3, column 3) suggest either an incompatibility between the chemical reactivity of the Cys side-chain and its presence in the paratope of antibodies, or its interference with the correct folding of a variable domain. For example, the mutant Cys residues could make erroneous disulphide bridges with the conserved Cys residues of the same variable domain. In this context, we observed that the least produced mutants were located seven to ten residues downstream of a conserved Cys residue, L-His30 relative to L-Cys23, H-Tyr32 relative to H-Cys22, and H-Arg99 relative to H-Cys92 (Table 3, column 4).

We observed that the molecules of scFvD1.3 (L-S93C) were mostly (82%) inactive. In contrast, the molecules of the scFv(L-S93ANBD) conjugate were mostly (86%) active (Table 6). Thus, the mild reduction of scFv(L-S93C) and the coupling of IANBD seemed to act as sieves and enrich the preparations in functional molecules. We assume that the misfolded molecules of scFv(L-S93C) were more sensitive than the properly folded ones to an attack of their disulphide bridges by 2-mercaptoethanol and IANBD, leading to their precipitation. The overall yield of construction of the conjugate from scFv(L-S93C) was 43% ($9 \times 86/18$; see Tables 3 and 6) when only the functional molecules were taken into account. Similar observations were made with other conjugates.

Validity of the design rules

We chose ten sites of scFvD1.3 to construct fluorescent conjugates, using the available structural and functional data. We considered that a conjugate was HEL sensitive if the maximal variation of fluorescence intensity between its HEL free and bound states satisfied $E > 10\%$. We considered that it was operational if, in addition, its affinity for HEL was not strongly affected relative to that of the wild-type ($\Delta\Delta G \leq 0.8$ kcal mol^{-1}). Five of the six conjugates which we constructed from residues of V_L were operational, and one of the four conjugates constructed from V_H. The results were different for the control sites. Among the two sites of scFvD1.3 which were strongly and directly involved in the interaction with HEL ($\Delta\Delta G \geq 2.3$ kcal mol^{-1} for one of the mutations; >62% of the side-chain ASA becomes buried on HEL binding), L-Trp92 gave a HEL-sensitive conjugate ($E = 55\%$) whereas L-Tyr50 gave an insensitive conjugate ($E = 1\%$). Thus, a strong involvement of the coupling residue in the interaction between antibody and antigen did not guarantee that the corresponding conjugate was antigen-sensitive. Out of the four scFvD1.3 sites which were located in an enlarged neighbourhood of HEL, only L-Asn31 gave an HEL-sensitive

conjugate (Table 3). Thus, the coupling sites can be searched for in priority within a narrow neighbourhood of the antigen, typically defined by a sphere of solvent with $r < 2.0$ Å. The Gly residues did not give HEL-sensitive conjugates, whether their C^{α} atom was buried (as H-Gly53) or exposed to the solvent (H-Gly31).

We took the prior mutagenesis data on FvD1.3 into account to design the sites of fluorophore coupling. The mutations of the chosen sites affected little the free energy of interaction between FvD1.3 and HEL ($\Delta\Delta G \leq 0.8$ kcal mol^{-1}; Table 1). We found that this energy of interaction was close for scFvD1.3(wt), the Cys mutants ($\Delta\Delta G \leq 0.8$ kcal mol^{-1}; Table 4), and the scFvD1.3–ANBD conjugates ($\Delta\Delta G \leq 0.4$ kcal mol^{-1}; Table 5) characterized here. Thus, the change of the fluorophore environment on binding of HEL had no significant energetic cost. The results suggested that the flexible aliphatic arm of IANBD allowed the fluorophore to occupy a position which did not obstruct the interface between antibody and antigen.

We used residue L-Trp92 of scFvD1.3 as a control site. This residue is directly and strongly involved in the interaction with HEL (Table 1). We found that mutation L-W92C decreased the energy of interaction strongly between scFvD1.3 and HEL ($\Delta\Delta G \geq 3$ kcal mol^{-1}), and that the coupling of IANBD did not restore it (Tables 4 and 5). Thus, there was no advantage, for scFvD1.3, in using an aromatic and energetically important residue as a coupling site, since other residues gave conjugates with as high E values (e.g. L-Ser93 and L-Thr94), or even higher E values (L-Tyr49) than L-Trp92, without compromising the affinity for HEL.

In summary, our structural and functional rules of design for the coupling site of the fluorophore were 60% reliable (6/10 predicted sites giving operational conjugates) and they guaranteed that the resulting fluorescent conjugate possessed the same parameters of interaction with the antigen as the parental antibody. The fact that we could obtain six different operational conjugates from scFvD1.3 and simple rules of design suggests strongly that the success of our approach did not depend on the experimental model and that it will be possible to transpose it to other antibodies (see the last paragraph of Discussion). Obviously, there is a choice of residues in a given binding site from which it is possible to make operational conjugates.

Coupling yields and accessibility of the γ-atoms

We modelled the structure of each scFvD1.3 mutant and calculated the CSA value for the S^{γ} atom of the mutant Cys residue. We did not find any relation between the CSA of the mutant S^{γ} atom and the efficiency of coupling with IANBD under our experimental conditions. For example, the scFvD1.3(L-Y49C) and scFvD1.3-(H-Y32C) mutants could be fully coupled with IANBD, even though their mutant S^{γ} atom was only 11% to 13% accessible to the solvent. The results suggested that the internal dynamics of scFvD1.3 enabled the reaction between the reactive fluorophore and the thiol group, even when the latter was only partially exposed. Whether the third criteria of choice for the coupling sites, i.e. the accessibility of the mutant S^{γ} atom, is necessary or superfluous for more rigid scFv fragments or other types of receptors, remains to be established.

The changes of Gly to Cys were more complex to analyse since there was no direct means to estimate the CSA of the mutant S^{γ} atom. The C^{α} atom of residue H-Gly31 is accessible to the solvent (CSA = 24.1%) whereas the C^{α} atom of H-Gly53 is totally buried. We found that IANBD was coupled efficiently ($\geq$100%) in position H-31 and inefficiently (42%) in position H-53. In the case of a Gly residue, the CSA of its C^{α} atom could thus provide some indication of the orientation of the Cys side-chain, added by mutation, at the surface of the scFv and on its availability for coupling.

Variation of fluorescence and position of the fluorophores

The residues of FvD1.3 that gave the most efficient conjugates from the viewpoint of the signal variation, E, were in direct contact with HEL in the structure of the FvD1.3:HEL complex or in contact by the intermediate of a water molecule (Table 3, columns 2 and 7). The value of E decreased when the distance between the coupling residue and HEL increased. In most cases, the value of E was positive, i.e. the binding of HEL increased the fluorescence intensity of the conjugate. These results were consistent with a partial protection of the coupled fluorophore by the binding of HEL against a dynamic quenching by the solvent.[26]

The value of E for the scFvD1.3 conjugates was equal to 75% at most under our experimental conditions, whereas the relative variation of the fluorescence intensity for the transfer of IANBD from water to ethanol was 500% for the same excitation and emission wavelengths. Therefore, the construction of conjugates from peripheral sites of coupling did not exploit the full sensitivity of IANBD to its environment. Larger values of E might be obtained by coupling the fluorophore at the centre of the antibody paratope, where the change of environment on binding of the antigen would be more drastic. However, a coupling at the centre of the paratope would modify the interaction between the scFv fragment and its antigen, lower their affinity and increase the detection threshold for the antigen. We could dose HEL with detection thresholds as low as 10 nM and 3 nM for the conjugates constructed from residues L-Ser93 (this work) and L-Thr94 (not shown), respectively. Therefore, the construction of conjugates

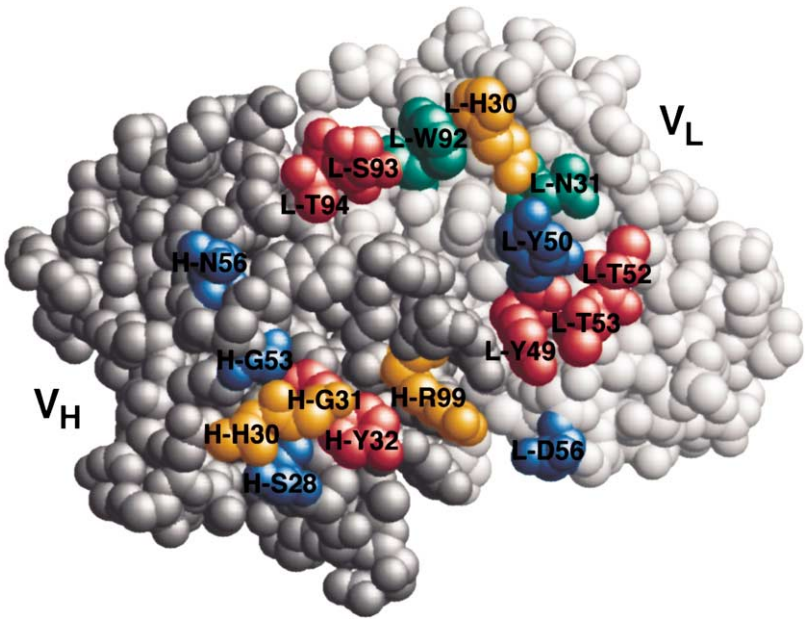

Figure 4. Position of the coupling sites in the structure of the free FvD1.3 fragment. Light grey, V_L; medium grey, V_H; red, residues which satisfied the design rules and gave operational conjugates ($E > 10\%$); yellow, satisfied the design rules but $E < 10\%$; green, control sites with $E > 10\%$; blue, controls with $E < 10\%$. The structure is seen from the viewpoint of HEL.

from peripheral sites appears as the most efficient strategy (Figure 4).

Prediction of peripheral sites without structural data

Numerous mutagenesis data are available on the FvD1.3 fragment (Table 1). We considered that a residue of FvD1.3 was functionally important if the free energy of interaction between FvD1.3 and HEL, ΔG, varied by more than 0.8 kcal mol^{-1} for at least one of its mutations. We considered that a fluorescent conjugate of scFvD1.3 was operational if it was HEL-sensitive ($E > 10\%$) and if its affinity for HEL was close to that of the parental scFvD1.3 fragment ($\Delta\Delta G < 0.8$ kcal mol^{-1}). We compared the positions of the residues which were functionally important and those which gave operational conjugates, along the sequence of scFvD1.3 (Figure 5). This comparison showed that the operational conjugates derived in majority from residues which were close to a functionally important residue ($\Delta\Delta G > 0.8$ kcal mol^{-1}) along the sequence, or which had themselves a weak functional importance ($0.5 < \Delta\Delta G < 0.8$ kcal mol^{-1}). The first set included L-Asn31, L-Tyr49, L-Thr52, L-Ser93 and L-Thr94; the second set included L-Tyr49 and H-Tyr32. Sequence and function data could thus be sufficient to choose peripheral coupling sites in the absence of structural data on the complex between antibody and antigen. Obtaining such data is easier and faster than a crystallographic study at high resolution, especially if combinatorial alanine scanning is used.[27] Thus, the transformation of an antibody fragment into a fluorescent immuno-conjugate appears possible even in the absence of any structural data. We are currently testing these assumptions.

The residues which gave operational conjugates, were located in the hypervariable structural loops, except L-Thr49 and L-Thr53, which were immediately adjacent to loop L2 (residues 50–52) but outside of it. These residues had Ser, Thr, Asn or Tyr side-chains, which were polar and thus had a high probability of being oriented towards the solvent or of establishing contacts with the antigen. It thus seems possible to target the construction of fluorescent conjugates on a limited number of CDR residues, initially on the sole basis of the sequence and in the absence of any structural or functional data. In this case, a screening of the potential sites by mutagenesis to Cys could provide both functional data and the mutations necessary for the coupling of the fluorophore.

Conclusions

From the crystal structure of the FvD1.3:HEL complex, we identified residues of FvD1.3 which are not involved in the binding of HEL but whose environment is modified upon binding. We changed these residues to Cys, then developed a method to couple a fluorophore to the free Cys residue efficiently and without denaturing the scFv fragment. Finally, we showed that the titration of HEL by the scFvD1.3(L-S93ANBD) conjugate could be specifically monitored by its fluorescence in a complex mixture like calf serum. Thus, the scFv conjugates had the constituent properties of reagentless fluorescent immuno-sensors. The same approach could be used with other types of receptors.

We will extend our approach to antibodies of unknown structure. The type of immuno-sensor that we describe here, would then constitute a new generation of analytical tools to detect and quantify antigenic molecules. Methods have been described to immobilize proteins, in a functional form and in arrays, on glass micro-slides and thus

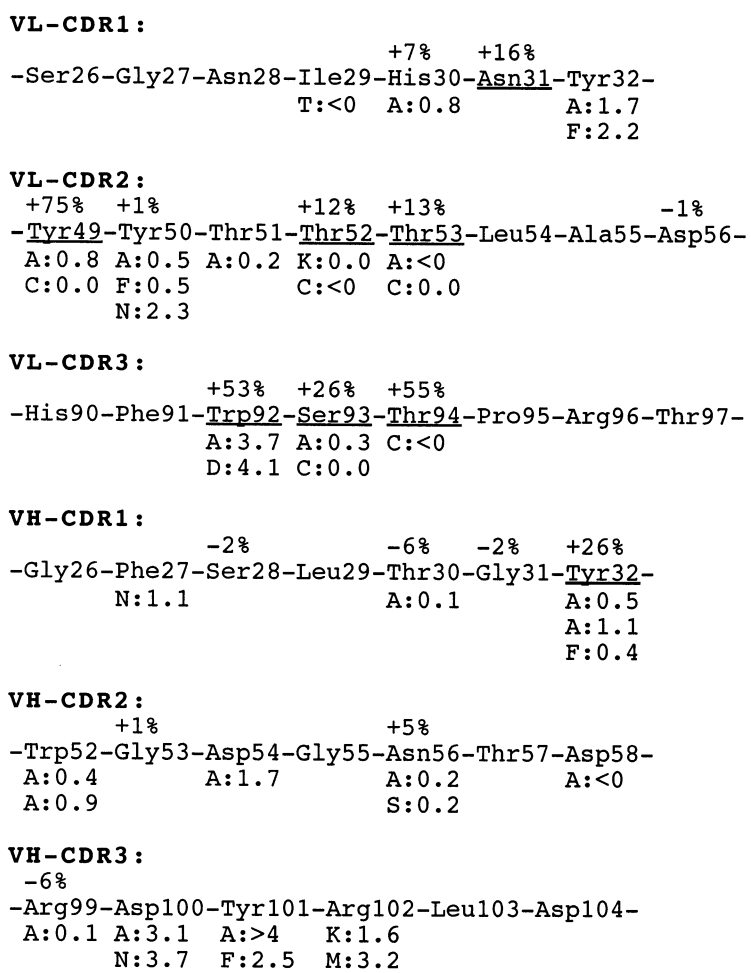

Figure 5. Comparison between the sites chosen for coupling and the sites important for the binding of HEL. Above the residues, relative variation of the conjugate fluorescence between its free and HEL bound states ($E_{535\ nm}$ in %; see Table 3). Underlined residues, positions for which $E > 10\%$. Under the sequence, known mutations with the corresponding $\Delta\Delta G$ values for the interaction with HEL (kcal mol^{-1}; see Tables 1 and 4).

detect a large number of fluorescent ligands simultaneously.[28] It was also reported that benzopyrene tetrol, a fluorescent aromatic compound, can be titrated intracellularly with an antibody immobilized at the tip of an optical nano-fibre.[29] As the immuno-sensors that we propose, do not require the antigen to possess any intrinsic optical property, they would greatly generalize these methods. The use of time-resolved fluorescence (time or frequency-domain methods) and evanescent-wave fluorescence should enable us to perform the measurements in turbid media and to increase the sensitivity of detection.[26]

Materials and Methods

Materials

SB medium and PBS buffer,[30] the *E. coli* strain HB2151,[31] and phagemid pASK98-D1.3[32] have been described. Buffer A was 500 mM NaCl, 20 mM Tris–HCl, (pH 7.9); buffer B, 150 mM NaCl, 50 mM Tris–HCl, (pH 7.5); buffer C, 150 mM NaCl, 50 mM sodium phosphate, (pH 7.0); buffer D, 0.005% (v/v) Tween 20, 150 mM NaCl, 10 mM Hepes, (pH 7.4); buffer E, 0.005% (v/v) Tween 20 in PBS. Hen egg white lysozyme (HEL), turkey egg lysozyme (TEL), and calf serum were purchased from Sigma; fluorophores and phosphines (Tris-cyanoethylphosphine, Tris-carboxyethylphosphine) from Molecular Probes Inc. The serum was filtered through a Millex GV cartridge (0.22 μm pore) before use.

Recombinant DNA procedures

Phagemid pMR1 codes for a single-chain Fv of mAbD1.3: V_H–$(Gly_4Ser)_3$–VL–His_6. pMR1 was derived from pASK98-D1.3 by introducing a DNA cassette, coding for Leu-Glu-His_6, between its *Xho*I and *Hin*dIII restriction sites. This cassette was formed by hybridization of two oligonucleotides: 5′-TCGAGATCAAGCGGCCGCTGGAACACCATCACCATCACCATTA-3′ and 5′-AGCTTAATGGTGATGGTGATGGTGTTCCAGCGGCCGCTTGATC-3′. Oligonucleotide site-directed mutagenesis was performed as described, using the DNA of pMR1 as template.[33] The DNA sequences of the mutated genes were verified.

Protein production and purification

The wild-type and mutant scFvD1.3 fragments were produced from plasmid pMR1 and its mutant derivative in strain HB2151. The bacterial cultures were grown at 22°C in SB medium for three generations until $A_{600\ nm} = 1.80$, and then induced for two hours with 0.22 μg/ml anhydrotetracycline (Sigma). The following steps were performed at 4 °C. The cells were pelleted by centrifugation, resuspended in buffer A with 1 mg/ml Polymyxin B Sulfate (ICN) and 5 mM imidazole (25 ml

for one litre of initial culture), stirred for 30 minutes and then centrifuged 30 minutes at 30,000*g*. The supernatant (periplasmic fluid) was treated with DNase I and loaded on a Ni-NTA column (Qiagen, 0.33 ml of resin for one litre of initial culture). The bound scFvD1.3 molecules were washed with 40 mM imidazole (20 volumes of resin) then eluted with 100 mM imidazole in buffer A. The yield of purified scFvD1.3 varied with each mutant and was comprised between 0.06 and 0.6 mg/l of culture medium.

Size-exclusion chromatography

The oligomeric states of the scFvD1.3 derivatives (40 μg/ml, 200 μl) were analysed by size exclusion chromatography on a Superdex 75 HR10/30 column (Pharmacia), in buffer B, at room temperature, and at a flow rate of 0.5 ml/minute. Chymotrypsinogen (M_r = 25.0 kDa) and bovine serum albumin (M_r = 67.2 kDa) were used as standards.

Mass spectrometry

scFvD1.3(wt) and scFvD1.3(VL-S93C) were dialysed extensively against 65 mM ammonium carbonate (pH 9.5) and then lyophilized. The scFvD1.3(S93-ANBD) conjugate was dialysed against 65 mM ammonium acetate (pH 5.0), because the fluorophore could uncouple at basic pH, and then lyophilised in the dark. Samples were dissolved in water/methanol/formic acid (50:45:5, by volume) and introduced into an API 365 triple-quadrupole mass spectrometer (Sciex, Thornill, Canada) at 5 μl/minute with a syringe pump. The ion source was used under positive mode. It comprised an electrospray interface which was pneumatically assisted and functioned at atmospheric pressure. The tip of the ion-spray probe and the orifice were held at 4.5 kV and 40 V, respectively. The mass spectrometer was scanned continuously from m/z 1100 to 1900 with a scan step of 0.1, a dwell time of 2.0 ms per step, and thus a scan duration of 16 seconds. Ten scans were averaged for each analysis. The calibration of the spectrometer was performed by matching ions of polypropylene glycol to known reference masses, stored in a calibration table. The data were processed with Biotoolbox 2.3 software (Sciex).

Fluorophore coupling

The mutants of scFvD1.3 were partially reduced with varying concentrations of 2-mercaptoethanol (0.1–50 mM) for one hour at room temperature, then transferred into buffer C with a HiTrap Desalting column (Pharmacia). A thiol-reactive fluorophore was added in a 20:1 molar excess over the scFv, and the reaction was carried out overnight at room temperature. The denatured proteins were removed by centrifugation for 30 minutes at 10,000 *g*, 4 °C, and the unreacted fluorophore was separated from the scFv by purification on Ni-NTA resin in buffer A. The protein yield was obtained by measuring the absorbances of the soluble protein fraction before and after the entire coupling procedure, with a Perkin–Elmer Lambda-2 split-beam spectrophotometer. The coupling yield was obtained by measuring the absorbances of the protein and fluorophore portions of the resulting biosensor. We took $\varepsilon_{280\ nm} = 51.13\ mM^{-1}$ for scFvD1.3 and its derivatives, calculated as described;[34] $\varepsilon_{280\ nm} = 2.12\ mM^{-1}$ and $\varepsilon_{500\ nm} = 31.8\ mM^{-1}$ for IANBD, $\varepsilon_{336\ nm} = 9.6\ mM^{-1}$ for CNBD, $\varepsilon_{492\ nm} = 75\ mM^{-1}$ for 5-IAF, $\varepsilon_{391\ nm} = 20\ mM^{-1}$ for acrylodan, measured with conjugates between the fluorophores and 2-mercaptoethanol (see Table 2 for abbreviations).

Fluorescence assays

Fluorescence was measured at 25 °C with a Perkin–Elmer LS-5B luminescence spectrometer, including the Rhodamine 101 dye as an internal reference. The excitation and emission slit widths were equal to 5 and 20 nm, respectively. IANBD, CNBD, 5-IAF and Acrylodan were excited at 480, 432, 492 and 391 nm, respectively. The fluorescence of the scFvD1.3 conjugates (0.5–1.5 μM) was measured before and after formation of a complex with a saturating concentration of lysozyme (20 μM), directly in the buffer used for the elution of the conjugate from the Ni-NTA column (100 mM imidazole in buffer A). scFv(L-S93ANBD) (500 nM in buffer B or 1 μM in serum) was titrated with increasing concentrations of lysozyme. The following equation was fitted to the experimental data:

$$Y = Y_p \cdot [P]_o + (Y_{pl} - Y_p) \cdot (K_D + [P]_o + x - ((K_D + [P]_o + x)^2 - 4x \cdot [P]_o)^{1/2})/2$$

where Y is the total fluorescence emission at 535 nm; $[P]_o$ and x, the total concentrations of active conjugate and antigen in the reaction, respectively; Y_p and Y_{pl}, the molar fluorescence of the free conjugate and of its complex with the antigen respectively; and K_D, the dissociation constant of the complex between the conjugate and the antigen.

Measurement of active concentrations by Biacore

The interactions between the scFvD1.3 derivatives and lysozyme were characterized with the Biacore 2000 apparatus (Biacore, Upsala, Sweden), at 25 °C. The active concentration of the wild-type scFvD1.3 in a purified preparation was obtained by measuring its initial rate of binding to immobilized HEL at different flow rates, under conditions of partial mass transport limitation.[35,36] Dilutions of this preparation (10 μl, 2.5–90 nM active sites) were then injected at a constant flow rate (10 μl/minute) on a surface of HEL, immobilized at high density, to establish a calibration curve, giving the initial rate of binding as a function of the active concentration.[37] Finally, the calibration curve was used to measure the active concentrations of the scFvD1.3 derivatives. The method is valid as long as the conditions of mass transport limitation are fulfilled.

Kinetic measurements by Biacore

The kinetics were performed with CM5 sensor chips (Biacore) comprising four flow cells. Cell 1 was used as a reference, i.e. no ligand was immobilized on the corresponding surface. Low densities of lysozyme (30–50 resonance units, RU) were immobilized in cells 2 and 3. The maximal response of the corresponding surfaces on injection of scFvD1.3 was between 30 and 100 RU. High densities of HEL (typically 3000 RU) were immobilized on the surface of cell 4 for measurement of the active concentrations. Solutions of the scFvD1.3 derivatives at five different concentrations (60 μL, 0.5–50 nM) were injected on flow cells 1, 2 and 3 at a flow rate of 30 μL/

minute. The dissociation was followed during three minutes in buffer D. The active concentration of each scFvD1.3 solution was measured with cell 4 immediately before the kinetic run. This procedure minimizes errors due to possible inactivation of the scFv fragment over time.[38] The kinetic parameters were calculated by a procedure of global fitting, as implemented in the BIAevaluation 3.0 software (Biacore). The values of the statistical parameter χ^2 were typically below 5% of the maximal response.

Competition Biacore

The competition experiments were performed either in buffer E or in calf serum. High densities of HEL (1000 RU) were immobilized on the surface of a CM5 sensor chip for measurement of the concentrations. A scFvD1.3 derivative, at a final concentration of 2 to 5 nM, was mixed in solution with either HEL or TEL at variable concentrations, and the reaction was left more than five hours at 25 °C to reach equilibrium. Each reaction mixture was injected at three different flow rates (15, 25 and 50 μl/minute) on the sensor chip. The concentration of free scFv was assumed to be proportional to its rate of capture by immobilized HEL (see above). The captured scFv represented $<7\%$ of the free scFv so that it did not shift the equilibrium of the reaction mixture. For the experiments in serum, the signal of the serum alone was substracted from the signal of the reaction mixture. The general quadratic equation of equilibrium was fitted directly to the raw experimental data, using K_D as a fitting parameter, as described.[39] The results were independent of the flow rate.

Analysis of the crystal structures

The structure of the complex between FvD1.3 and HEL (PDB 1vfb)[12] was analysed with the WHAT IF program.[40] The solvent accessible and contact surface areas (ASA and CSA) were calculated with the ACCESS routine. They were expressed as percentages of the ASA or CSA for the same atom or residue in a Gly-*X*-Gly context. The CSA was calculated with a solvent sphere of radius 1.4 Å.

Acknowledgements

We thank Homme Hellinga for bringing this interesting subject to our attention and Shamila Naïr for critical reading of the manuscript, Arne Skerra for pASK98-D1.3, and Jean-Claude Rousselle for mass-spectrometry. This research was funded by grants from the Ministry of National Education, Research and Technology (programme for fundamental research in microbiology, infectious and parasitic diseases) and from the Ministry of Defense (contract 99 34 043/DSP/STTC).

References

1. Lowe, C. R. (1984). Biosensors. *Trends Biotechnol.* **2**, 59–65.
2. Morgan, C. L., Newman, D. J. & Price, C. P. (1996). Immunosensors: technology and opportunities in laboratory medicine. *Clin. Chem.* **42**, 193–209.
3. North, J. R. (1985). Immunosensors: antibody-based biosensors. *Trends Biotechnol.* **3**, 180–186.
4. Pollack, S. J., Nakayama, G. R. & Schultz, P. G. (1988). Introduction of nucleophiles and spectroscopic probes into antibody combining sites. *Science*, **242**, 1038–1040.
5. Brune, M., Hunter, J. L., Corrie, J. E. & Webb, M. R. (1994). Direct, real-time measurement of rapid inorganic phosphate release using a novel fluorescent probe and its application to actomyosin subfragment 1 ATPase. *Biochemistry*, **33**, 8262–8271.
6. Gilardi, G., Zhou, L. Q., Hibbert, L. & Cass, A. E. (1994). Engineering the maltose binding protein for reagentless fluorescence sensing. *Anal. Chem.* **66**, 3840–3847.
7. Marvin, J. S. & Hellinga, H. W. (1998). Engineering biosensors by introducing fluorescent allosteric signal transducers: construction of a novel glucose sensor. *J. Am. Chem. Soc.* **120**, 7–11.
8. Sloan, D. J. & Hellinga, H. W. (1998). Structure-based engineering of environmentally sensitive fluorophores for monitoring protein–protein interactions. *Protein Eng.* **11**, 819–823.
9. Glockshuber, R., Schmidt, T. & Pluckthun, A. (1992). The disulphide bonds in antibody variable domains: effects on stability, folding in vitro, and functional expression in *Escherichia coli*. *Biochemistry*, **31**, 1270–1279.
10. Johnson, G. & Wu, T. T. (2001). Kabat database and its applications: future directions. *Nucl. Acids Res.* **29**, 205–206.
11. Biocca, S., Ruberti, F., Tafani, M., Pierandrei-Amaldi, P. & Cattaneo, A. (1995). Redox state of single chain Fv fragments targeted to the endoplasmic reticulum, cytosol and mitochondria. *Biotechnology (NY)*, **13**, 1110–1115.
12. Bhat, T. N., Bentley, G. A., Boulot, G., Greene, M. I., Tello, D., Dall'Acqua, W. *et al*. (1994). Bound water molecules and conformational stabilization help mediate an antigen–antibody association. *Proc. Natl Acad. Sci. USA*, **91**, 1089–1093.
13. Hawkins, R. E., Russell, S. J., Baier, M. & Winter, G. (1993). The contribution of contact and non-contact residues of antibody in the affinity of binding to antigen. The interaction of mutant D1.3 antibodies with lysozyme. *J. Mol. Biol.* **234**, 958–964.
14. Ito, W., Iba, Y. & Kurosawa, Y. (1993). Effects of substitutions of closely related amino acids at the contact surface in an antigen–antibody complex on thermodynamic parameters. *J. Biol. Chem.* **268**, 16639–16647.
15. Ysern, X., Fields, B. A., Bhat, T. N., Goldbaum, F. A., Dall'Acqua, W., Schwarz, F. P. *et al*. (1994). Solvent rearrangement in an antigen–antibody interface introduced by site-directed mutagenesis of the antibody combining site. *J. Mol. Biol.* **238**, 496–500.
16. Dall'Acqua, W., Goldman, E. R., Eisenstein, E. & Mariuzza, R. A. (1996). A mutational analysis of the binding of two different proteins to the same antibody. *Biochemistry*, **35**, 9667–9676.
17. England, P., Bregegere, F. & Bedouelle, H. (1997). Energetic and kinetic contributions of contact residues of antibody D1.3 in the interaction with lysozyme. *Biochemistry*, **36**, 164–172.
18. Dall'Acqua, W., Goldman, E. R., Lin, W., Teng, C., Tsuchiya, D., Li, H. *et al*. (1998). A mutational analysis of binding interactions in an antigen–antibody protein–protein complex. *Biochemistry*, **37**, 7981–7991.

19. England, P., Nageotte, R., Renard, M., Page, A. L. & Bedouelle, H. (1999). Functional characterization of the somatic hypermutation process leading to antibody D1.3, a high affinity antibody directed against lysozyme. *J. Immunol.* **162**, 2129–2136.
20. Holliger, P., Prospero, T. & Winter, G. (1993). Diabodies: small bivalent and bispecific antibody fragments. *Proc. Natl Acad. Sci. USA*, **90**, 6444–6448.
21. Braden, B. C., Fields, B. A., Ysern, X., Goldbaum, F. A., Dall'Acqua, W., Schwarz, F. P. *et al*. (1996). Crystal structure of the complex of the variable domain of antibody D1.3 and turkey egg white lysozyme: a novel conformational change in antibody CDR-L3 selects for antigen. *J. Mol. Biol.* **257**, 889–894.
22. Al-Lazikani, B., Lesk, A. M. & Chothia, C. (1997). Standard conformations for the canonical structures of immunoglobulins. *J. Mol. Biol.* **273**, 927–948.
23. Chothia, C., Lesk, A. M., Gherardi, E., Tomlinson, I. M., Walter, G., Marks, J. D. *et al*. (1992). Structural repertoire of the human VH segments. *J. Mol. Biol.* **227**, 799–817.
24. Tomlinson, I. M., Cox, J. P., Gherardi, E., Lesk, A. M. & Chothia, C. (1995). The structural repertoire of the human V_κ domain. *EMBO J.* **14**, 4628–4638.
25. Shirai, H., Kidera, A. & Nakamura, H. (1999). H3-rules: identification of CDR-H3 structures in antibodies. *FEBS Letters*, **455**, 188–197.
26. Lakowicz, J. R. (1999). *Principles of Fluorescent Spectroscopy*, 2nd edit., Kluwer Academic/Plenum, New York.
27. Weiss, G. A., Watanabe, C. K., Zhong, A., Goddard, A. & Sidhu, S. S. (2000). Rapid mapping of protein functional epitopes by combinatorial alanine scanning. *Proc. Natl Acad. Sci. USA*, **97**, 8950–8954.
28. MacBeath, G. & Schreiber, S. L. (2000). Printing proteins as microarrays for high-throughput function determination. *Science*, **289**, 1760–1763.
29. Vo-Dinh, T., Alarie, J. P., Cullum, B. M. & Griffin, G. D. (2000). Antibody-based nanoprobe for measurement of a fluorescent analyte in a single cell. *Nature Biotechnol.* **18**, 764–767.
30. Sambrook, J., Fritsch, E. F. & Maniatis, T. (1989). *Molecular Cloning: A Laboratory Manual*, Cold Spring Harbor Laboratory Press, Cold Spring Harbor, NY.
31. Carter, P., Bedouelle, H. & Winter, G. (1985). Improved oligonucleotide site-directed mutagenesis using M13 vectors. *Nucl. Acids Res.* **13**, 4431–4443.
32. Skerra, A. (1994). Use of the tetracycline promoter for the tightly regulated production of a murine antibody fragment in *Escherichia coli*. *Gene*, **151**, 131–135.
33. Kunkel, T. A., Roberts, J. D. & Zakour, R. A. (1987). Rapid and efficient site-specific mutagenesis without phenotypic selection. *Methods Enzymol.* **154**, 367–382.
34. Pace, C. N., Vajdos, F., Fee, L., Grimsley, G. & Gray, T. (1995). How to measure and predict the molar absorption coefficient of a protein. *Protein Sci.* **4**, 2411–2423.
35. Christensen, L. L. (1997). Theoretical analysis of protein concentration determination using biosensor technology under conditions of partial mass transport limitation. *Anal. Biochem.* **249**, 153–164.
36. Richalet-Secordel, P. M., Rauffer-Bruyere, N., Christensen, L. L., Ofenloch-Haehnle, B., Seidel, C. & Van Regenmortel, M. H. (1997). Concentration measurement of unpurified proteins using biosensor technology under conditions of partial mass transport limitation. *Anal. Biochem.* **249**, 165–173.
37. Karlsson, R., Fagerstam, L., Nilshans, H. & Persson, B. (1993). Analysis of active antibody concentration. Separation of affinity and concentration parameters. *J. Immunol. Methods*, **166**, 75–84.
38. Choulier, L., Laune, D., Orfanoudakis, G., Wlad, H., Janson, J., Granier, C. & Altschuh, D. (2001). Delineation of a linear epitope by multiple peptide synthesis and phage display. *J. Immunol. Methods*, **249**, 253–264.
39. Rondard, P., Goldberg, M. E. & Bedouelle, H. (1997). Mutational analysis of an antigenic peptide shows recognition in a loop conformation. *Biochemistry*, **36**, 8962–8968.
40. Vriend, G. (1990). WHAT IF: a molecular modeling and drug design program. *J. Mol. Graph.* **8**, 52–56.

Edited by I. A. Wilson

(Received 16 October 2001; received in revised form 23 January 2002; accepted 24 January 2002)